

Cite this: *RSC Sustainability*, 2024, 2, 1081

# A biomass hydrogel solar evaporator based on low-grade tobacco leaves for water evaporation and thermoelectric conversion applications†

Zuoyu Wang,<sup>a</sup> Lu Han,<sup>c</sup> Gaolei Xi,<sup>c</sup> Tao Jia,<sup>c</sup> \*<sup>ab</sup> Yi Liu,<sup>a</sup> Xiao He,<sup>a</sup> Hongxia Wang\*<sup>c</sup> and Bin Li\*<sup>ab</sup>

Interfacial solar-driven evaporation technology has attracted widespread attention. The core technology of photothermal conversion is photothermal materials and biomass photothermal materials are characterized by low cost, large specific surface area, environmental friendliness, and renewability. Low-grade tobacco leaves (LTLs) are harmful to the environment; however, they also have good recycling potential. In this work, a high-performance, low cost, and environmentally friendly solar steam generation material was fabricated by combining polyvinyl alcohol hydrogels and biomass photothermal material LTL. The photothermal conversion efficiency can reach 14.33% for LTL under sunlight irradiation, and the evaporation rate reached 1.07 kg m<sup>-2</sup> h<sup>-1</sup> with an evaporation efficiency of 74.3%. The waste heat generated during solar water evaporation can be effectively used for synergistic water-electricity cogeneration, thus achieving an evaporation rate and voltage of 0.83 kg m<sup>-2</sup> h<sup>-1</sup> and 38.7 mV under sunlight irradiation, respectively. This work enhances the prospects for the comprehensive utilization of biomass resources and provides effective application methods for the development of seawater desalination technology.

Received 9th January 2024  
Accepted 3rd March 2024

DOI: 10.1039/d4su00005f

rsc.li/rscsus

## Sustainability spotlight

In recent years, under the influence of climate issues, the construction of a clean, low-carbon, and efficient energy system has become a global consensus and inevitable trend. Solar energy is a type of renewable energy. Referring to solar thermal radiation energy, the main performance is often said to be sun rays. In modern times, it is commonly used to generate electricity or provide energy for water heaters. In addition, by 2025, the total consumption of biomass energy will reach 180 million tons of standard coal. Biomass energy should account for more than 14.5% of total renewable energy consumption. Increasing the development of biomass energy and promoting the industrialization process of the comprehensive utilization of biomass resources are important measures to implement the green development strategy and promote the construction of ecological civilization and sustainable development. In this work, a high-performance, low-cost, and environmentally friendly solar steam generation material was fabricated by combining polyvinyl alcohol (PVA) hydrogels and biomass photothermal material from low-grade tobacco leaves. The photothermal conversion efficiency can achieve 14.33% for abandoned tobacco leaves under sunlight irradiation, and the evaporation rate reached 1.07 kg m<sup>-2</sup> h<sup>-1</sup> with an evaporation efficiency of 74.3%. The waste heat generated during solar water evaporation can be effectively used for synergistic water-electricity cogeneration. This work enhances the prospects for the comprehensive utilization of biomass resources, provides effective application methods for the development of seawater desalination technology, and can also achieve sustainable energy utilization and reduce environmental pollution.

## 1 Introduction

Energy crises and the shortage of freshwater resource have attracted worldwide attention in the 21st century.<sup>1</sup> Therefore, there is an urgent need to implement a simple, efficient, and convenient approach for freshwater conversion.<sup>2,3</sup> At present, with the increasing demand for freshwater resources, many mature application technologies have been developed,<sup>4</sup> such as multi-stage flash evaporation,<sup>5</sup> multi effect distillation,<sup>6</sup> reverse osmosis,<sup>7</sup> nanofiltration method,<sup>8</sup> and electro dialysis.<sup>9</sup> Compared with other seawater desalination technologies, the sustainability and economic advantages of interfacial solar-driven photothermal evaporation make it an attractive

<sup>a</sup>Key Laboratory of Forest Plant Ecology, Ministry of Education, Engineering Research Center of Forest Bio-Preparation, Heilongjiang Provincial Key Laboratory of Ecological Utilization of Forestry Based Active Substances, College of Chemistry, Chemical Engineering and Resource Utilization, Northeast Forestry University, 26 Hexing Road, Harbin 150040, P. R. China. E-mail: jiataopolychem@nefu.edu.cn

<sup>b</sup>Post-doctoral Mobile Research Station of Forestry Engineering, Northeast Forestry University, Hexing Road 26th, Harbin, Heilongjiang 150040, P. R. China

<sup>c</sup>Technology Center for China Tobacco Henan Industrial Limited Company, Zhengzhou, Henan Province, 450000, P. R. China

† Electronic supplementary information (ESI) available. See DOI: <https://doi.org/10.1039/d4su00005f>



solution.<sup>10</sup> Interface solar steam generators capture solar energy and concentrate heat at the gas–liquid interface for efficient water evaporation. To obtain high photothermal conversion efficiency, many researchers have been continuously exploring and developing new photothermal materials. Numerous photothermal materials have been reported, mainly involving metal-based inorganic materials,<sup>11</sup> carbon-based inorganic materials,<sup>12</sup> organic-inorganic hybrid materials,<sup>13</sup> organic polymers,<sup>14,15</sup> and other small molecule materials.<sup>16</sup> In practice, these materials generally exhibit a relatively good performance.<sup>17</sup> However, these reported materials still have drawbacks such as low absorption efficiency and inevitable heat losses in solar energy, which result in low conversion and utilization efficiency of solar energy and a rapid increase in application costs.<sup>18</sup> This largely restricts the application range and large-scale use of photothermal technology. Biomass-based materials possess many advantages over photothermal materials, such as excellent biocompatibility, sustainability, and good stability.<sup>19</sup> Based on these characteristics, a biomass-based material was fabricated to have the potential to be an excellent photothermal material. Moreover, biomass-based materials are mostly composed of wood, algae, mushrooms, and straw.<sup>20</sup> They not only possess the above characteristics but also have the special characteristics of natural availability, renewability, and low cost. By utilizing biomass-based materials for membrane technology improvement and biomass waste for energy recovery, the energy consumption and environmental impact of seawater desalination can be reduced. This demonstrates that further research and development of innovative technologies and methods for biomass-based applications in seawater desalination is very meaningful and necessary.

Biomass-based materials contain many organic compounds, some of which have strong absorbance. Therefore, biomass-based materials are considered excellent photothermal materials for seawater desalination.<sup>21</sup> Inspired by this, low-grade tobacco leaves (LTL) were selected as the photothermal material in this study. Approximately 0.9 million tons to 1.5 million tons of tobacco in the world's annual tobacco production are discarded due to their inability to be used in cigarette production. These discarded tobacco leaves are collectively referred to as LTL. Simultaneously, the tobacco production and processing process generates tobacco leaf fragments and tobacco dust, and according to incomplete statistics, nearly 2 million tons of tobacco dust are generated annually. Although some LTL and tobacco residues are currently used in the production of tobacco flakes,<sup>22</sup> there are still a large number of LTL and tobacco residues that have not been fully utilized.<sup>23</sup> This not only caused certain pressure on the environment but also caused a serious waste of resources. Therefore, developing comprehensive utilization technologies for LTL and tobacco fragments is a major issue that the tobacco industry urgently needs to solve.<sup>24</sup>

A large amount of pigments are distributed in the LTL, which makes them have good light-absorbing properties. By analyzing the infrared range, it can be proven that the main components of light-absorbing pigments in LTL are carotenoids and chlorophyll.<sup>25</sup> Among them, chlorophyll is a necessary pigment for plants to carry out photosynthesis, which can convert light

energy into chemical energy.<sup>26</sup> In addition, due to the cooperative part of carotenoids, light absorption is further improved. On the one hand, carotenoids collect light and transmit it to chlorophyll. On the other hand, they are important antioxidants for reducing light damage and photoinhibition.<sup>27–29</sup> Besides, they can efficiently absorb light because of the dispersion of these light-absorbing components in LTL. For example, chlorophyll molecules are widely distributed in the chloroplasts of leaves, which allows lighter to be absorbed and converted into other forms of energy.

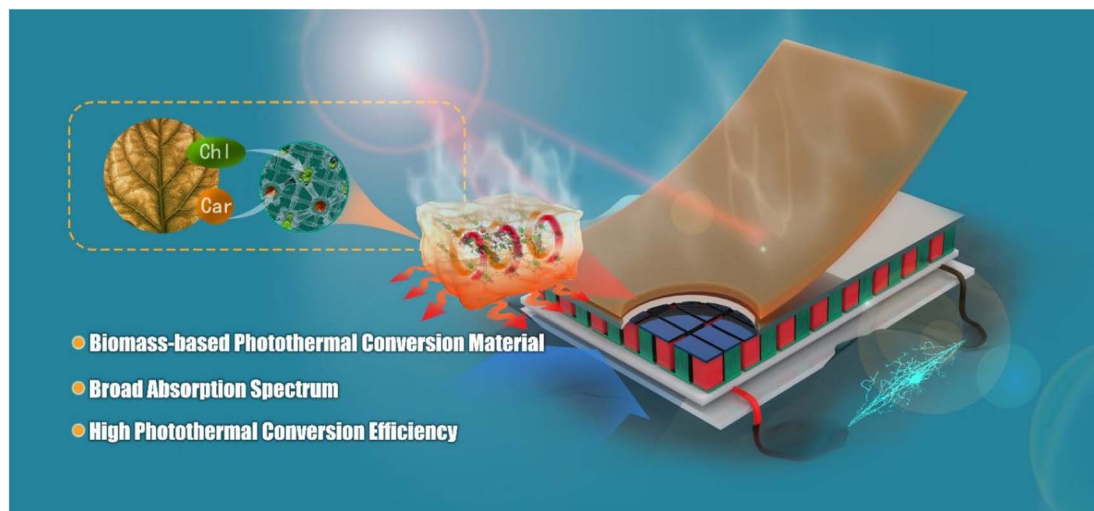
There is no doubt that an efficient and environmentally friendly method of photosynthesis converts solar energy into chemical energy, which is further converted into heat energy and releases heat from plants. Importantly, this thermal effect can be utilized to save energy and accelerate seawater desalination. Therefore, the development of biomass-based materials for water and electricity cogeneration has broad application prospects in the field of solar-driven seawater desalination.<sup>30</sup>

The core of solar-driven evaporation water technology is one of the photothermal materials and the other is the carrier. In the continuous development and innovation of technology,<sup>31,32</sup> hydrogel as a new evaporation carrier material has broad application prospects because of its low cost, efficient operation, and strong sustainability.<sup>33</sup> At present, researchers have successfully developed different types of hydrogel carriers, which show good application potential in evaporation technology, and some encouraging research results have been obtained.<sup>34</sup> Compared with traditional evaporation carriers, polyvinyl alcohol (PVA) hydrogel is a polymeric network with a three-dimensional porous structure, with a large surface area and numerous channels.<sup>35–37</sup> The hydrogel carrier possesses high water absorption capacity and good water retention. Moreover, the water in a PVA hydrogel has almost the same properties as bulk liquid water. Water easily escapes from the hydrogel surface and evaporates into the air, which can achieve a large amount of water evaporation in a relatively short time.

In this work, LTL powder was applied as biomass photothermal materials for photothermal conversion experiments (Scheme 1). Herein, to achieve a high-performance, low-cost, and ecofriendly device, using LTL powder as a photothermal material and PVA hydrogel as a water carrier, an LTL-based photothermal hydrogel was prepared. The results show that the low-grade tobacco leaves hydrogel (LTL/H) showed a broad absorption spectrum ranging from 300 to 1000 nm. The LTL powder has a high photothermal conversion efficiency of 14.33% under 1.0 kW m<sup>-2</sup> simulated solar irradiation. The water evaporation rate of LTL/H was 1.07 kg m<sup>-2</sup> h<sup>-1</sup> under 1.0 kW m<sup>-2</sup> simulated solar irradiation, and the water evaporation efficiency reached 74.3%.

Furthermore, the water and electricity co-generation device was constructed by applying LTL/H and thermoelectric modules to maximize the utilization of waste heat energy produced during evaporation, aiming to generate electricity based on temperature differences. The evaporation rate of the water-electric cogeneration device and the stable output voltage are 0.83 kg m<sup>-2</sup> h<sup>-1</sup> and 38.7 mV under solar irradiation, respectively. Based on the good experimental results, it is confirmed





Scheme 1 Schematic diagram of LTL/H for the co-generation of clean water and electricity.

that the complex formed by PVA hydrogel and LTL has superior photothermal conversion ability, which can be applied to seawater desalination. Simultaneously, the biomass-based hydrogel solar evaporator was designed to solve the situation of rapid growth in tobacco production and oversupply. This strategy for the comprehensive utilization of resources, energy conversion, and clean energy-related issues, implementing the use of biomass resources as photothermal materials for water and electricity integration, has a series of guiding significance.<sup>38</sup>

## 2 Results and discussion

### 2.1 Photothermal performance of low-grade tobacco leaves (LTL) powder

LTL are rich in many natural pigments, the most abundant of which are chlorophyll and carotenoids with a broad light-absorbance range.<sup>39</sup> Therefore, LTL have the potential to be an efficient photothermal material. LTL were ground into powder to study their photothermal properties. The UV-vis-NIR absorption spectrum of LTL powder exhibited wide absorbance in the range of 300–1000 nm (Fig. 1a). Furthermore, the photothermal properties of the LTL powder were evaluated. By analyzing the UV-vis-NIR absorption spectrum, the photothermal performance of simulated sunlight at different power densities was tested. By quickly recording temperature changes under an infrared thermal imager, it was found that under the condition of  $100 \text{ mW cm}^{-2}$ , the temperature rose to  $47.5 \text{ }^\circ\text{C}$  within 5 minutes (Fig. 1b). As the solar power density increases, the highest temperature at which the material rises also increases. At higher power densities ( $200 \text{ mW cm}^{-2}$ ), it can increase to  $80.1 \text{ }^\circ\text{C}$ , thereby exhibiting excellent photothermal behavior (Fig. 1c). In addition, simulating LTL powder under  $1.0 \text{ kW m}^{-2}$  irradiation for 5 h, it was found that the highest temperature of the material can increase to  $52 \text{ }^\circ\text{C}$  (Fig. 1d). Simultaneously, the temperature can still be maintained around  $52 \text{ }^\circ\text{C}$  after five light switching cycles, showing good photostability (Fig. 1e). The above experiments have

preliminarily demonstrated the excellent photothermal performance of LTL powder. To further confirm our inference, its photothermal conversion efficiency was studied.<sup>40</sup> The photothermal conversion efficiency of LTL powder dispersed in water is 14.33% under one sunlight irradiation. It can be observed that LTL is a good potential photothermal material for interfacial solar-driven photothermal evaporation (Fig. 1f).

### 2.2 Low-grade tobacco leaves hydrogel (LTL/H) for water evaporation performance

Based on the good photothermal conversion performance of LTL and the excellent water absorption capacity of polyvinyl alcohol (PVA) hydrogel, a solar vapor generation system combining LTL with PVA hydrogel was constructed. The LTL/H was prepared under agitation using 4% PVA and 50% glutaraldehyde (GLUT) at a ratio of 25 : 1 and mixed with fixed LTL powder. The concentrations of the PVA solutions were 4% (w/v). They were stirred at  $100 \text{ }^\circ\text{C}$  for 2 h and then cooled to room temperature. After that, GLUT was added, and the samples were stirred again for 2 h to promote cross-linking between the PVA chains. Then, a well-mixed solution was poured into a mold and set overnight at room temperature for molding. Subsequently, the obtained hydrogels were moved into a  $-20 \text{ }^\circ\text{C}$  environment, frozen for about 24 h, and then thawed at room temperature for 12 h for three consecutive cycles to fabricate physically cross-linking structures for further experiments. The use of molds to prepare hydrogels of different shapes showed that LTL/H exhibits high mechanical strength and greater stability (Fig. S1, ESI<sup>†</sup>). The hydrogels of various shapes can be fabricated into solar steam generation devices with specific functionalities. The surface wettability of LTL and LTL/H was measured (Fig. S2 and S3, ESI<sup>†</sup>), and the results showed that the water contact angles of LTL and LTL/H were both  $\approx 0^\circ$ , which confirmed that their hydrophilicity was good. Additionally, Scanning Electron Microscope (SEM) images of blank hydrogel and LTL/H show that the hydrogel had a porous network



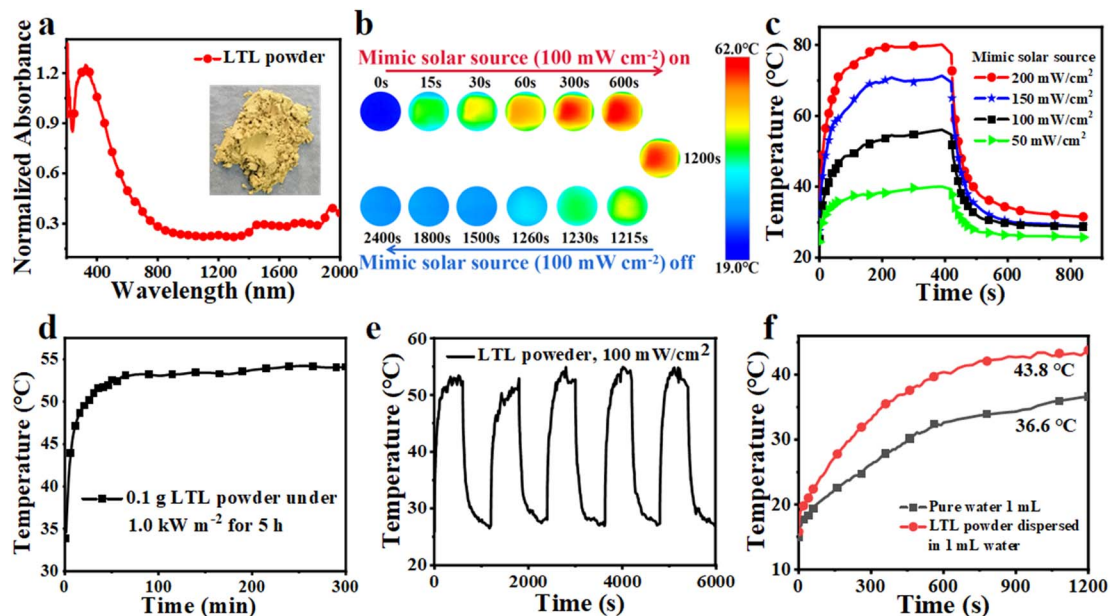


Fig. 1 (a) UV-vis-NIR absorption spectrum of the LTL powder. The illustration shows a digital photo of the LTL powder. (b) Infrared thermal images of LTL powder (0.1 g) under simulated solar energy ( $100 \text{ mW cm}^{-2}$ ) irradiation and after turning off the source. (c) Photothermal behavior of LTL powder under simulated solar irradiation at different power densities (50, 100, 150, and  $200 \text{ mW cm}^{-2}$ ). (d) Temperature changes in the LTL powder under  $1.0 \text{ kW m}^{-2}$  irradiation for 5 h. (e) Photobleaching resistance of the LTL powder during five heating and cooling cycles. (f) Temperature changes of 1 mL pure water and LTL powder dispersed in 1 mL pure water under one simulated solar irradiation.

structure (Fig. 2a and b). The pore size distribution ranges from 15–39  $\mu\text{m}$  for the blank hydrogel and 21–70  $\mu\text{m}$  for LTL/H. The reason for this is that the LTL powder entered the pore of the PVA hydrogel during the preparation of the LTL/H, resulting in a larger pore size. Moreover, it was found that the SEM image

showed that the LTL/H system surface was rougher than the pure hydrogel material surface, and this rough surface structure was conducive to light management and photon capture, which can lead to the promotion of light absorption and photothermal conversion of the surface. The photophysical properties of LTL/

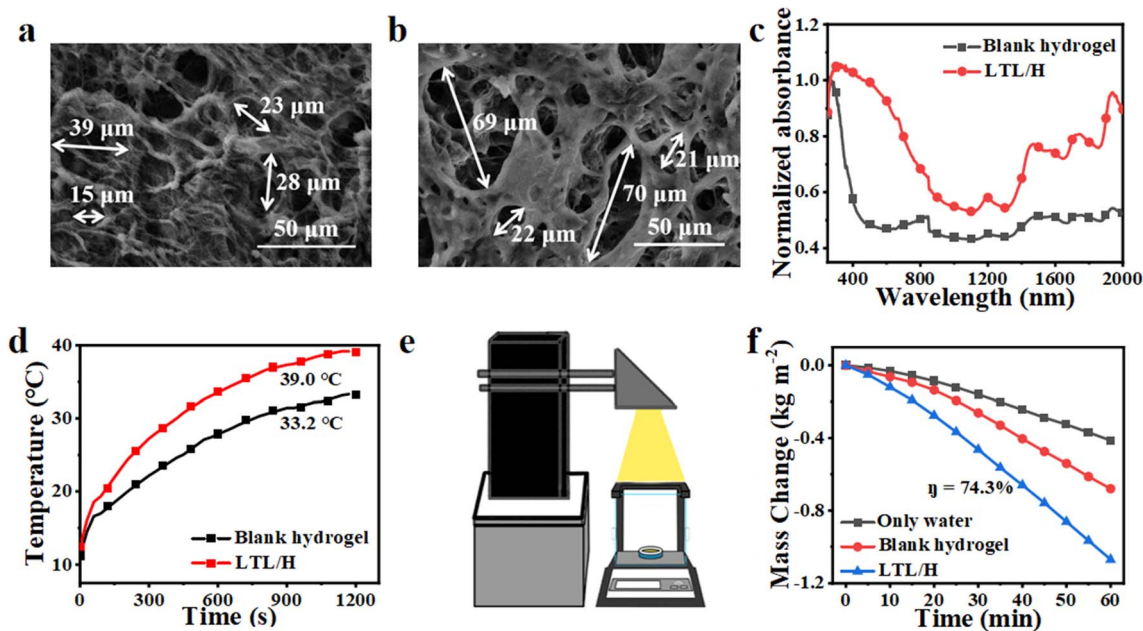


Fig. 2 (a) SEM image of the blank hydrogel. (b) SEM image of LTL/H. (c) UV-vis-NIR absorption spectra of blank hydrogel and LTL/H. (d) Surface heating ability of blank hydrogel and LTL/H under the irradiation of a solar light. (e) Schematic illustration of the solar evaporator. (f) Water evaporation rate diagram and efficiency diagram of LTL/H.



H were characterized by UV-vis-NIR absorption spectra, and the LTL/H showed a broad absorption spectrum of 300–1000 nm (Fig. 2c). The reflection spectra of LTL/H and blank hydrogel are also provided in Fig. S4, ESI.† The light reflection intensity of LTL/H is weaker than that of blank hydrogel, indicating that the light harvesting ability of PVA hydrogel with LTL is enhanced. The photothermal properties of LTL/H were studied next. As shown in Fig. 2d, under the irradiation of one sunlight, the surface temperature of the LTL/H rapidly increased and reached 39.0 °C within 20 minutes. Under the same conditions, it was higher than the surface temperature of the blank hydrogel, which proved that the introduction of LTL could effectively promote the evaporation of water.

Due to the excellent photothermal performance of LTL and the superior water supply performance of hydrogel, an eco-friendly and efficient solar-driven interfacial evaporation device was constructed (Fig. 2e). The whole used LTL powder as the photothermal layer of photothermal conversion and PVA hydrogel as the support carrier for water. The LTL/H evaporator is fixed with polystyrene (PS) foam in a plastic container filled with water. The solar-driven water evaporation rate and water evaporation efficiency were systematically studied, and the simulation equipment was used to measure the mass change varying with time under one solar irradiation in real time. The effective projection area is about 9.18 cm<sup>2</sup>. It is worth noting that the LTL/H with 0.30 g of LTL powder has a high water evaporation rate and good performance. The water evaporation rate of this material reaches 1.07 kg m<sup>-2</sup> h<sup>-1</sup>, and the water evaporation efficiency is  $\eta = 74.3\%$ . However, under the same environmental conditions, the evaporation efficiencies of pure water and blank hydrogel were only 28.5% and 47.1%, respectively (Fig. 2f), which are much lower than those of LTL/H, further proving the excellent water evaporation performance of LTL/H. The specific experimental method and calculation process are provided in the ESI.† To highlight the advantages of LTL, 0.02 g carbon black (CB) powder was mixed with 0.3 g LTL powder to prepare the hydrogel. By measuring the surface temperature and water evaporation performance, it was found that the surface temperature of the LTL + CB hydrogel (LTL + CB/H) increased from 12.2 °C to 39.2 °C within 20 minutes (Fig. S5, ESI†). The evaporation water rate was 1.15 kg m<sup>-2</sup> h<sup>-1</sup> with an efficiency of 80.0% (Fig. S6, ESI†) under sunlight irradiation. This confirmed that the water evaporation property of LTL/H with CB slightly increased. However, this work highlights the use of LTL without any treatment for photothermal conversion properties and its application in the field of water purification and energy conversion. Therefore, subsequent experiments are based on the material of the LTL.

### 2.3 LTL/H for water and electricity cogeneration

Solar-driven interfacial evaporation is a promising strategy for freshwater harvesting, as it harnesses both solar energy and water resources. To further enhance its efficiency, we develop a synergistic system that combines the LTL/H solar evaporator with thermoelectric power generation. Thermoelectric power generation technology is the use of thermoelectric materials

Seebeck effect to convert heat into electricity method. The Seebeck effect refers to the movement of electric charges due to the temperature difference when two conductors at different temperatures are connected, resulting in a voltage difference. The mathematical formula  $V = \alpha\Delta T$  calculates the voltage ( $V$ ) produced, where  $\alpha$  represents the Seebeck coefficient of the thermoelectric material (in V K<sup>-1</sup>) and  $\Delta T$  represents the temperature difference between the two surfaces of the generator.<sup>41</sup>

When a thermoelectric material is heated, the electrons in it are excited, creating a stream of electrons. This flow of electrons creates an electric field inside the material, which creates an electric potential difference. When two thermoelectric materials with different temperatures are joined together, the temperature difference causes electrons to flow from the hot side to the cold side, which generates an electric current. By connecting the thermoelectric material into a loop and introducing the current into an external circuit, the conversion of heat energy into electricity can be achieved.<sup>42</sup> Therefore, to fully utilize the waste heat generated by solar-driven interface evaporation, a solar-driven water-electricity integrated generation device is designed, as shown in Fig. 3a. This integrated water-electricity generation system helps address the current water-energy challenges, surpassing the limitations of traditional single-source energy conversions, thereby supporting sustainable development. In the study, the LTL/H cut to a size consistent with the shape of the thermoelectric module (area  $\approx 16$  cm<sup>2</sup>) is coated on the upper surface of the thermoelectric module (TE module), and both LTL/H end in contact with water; a PS foam frame is used to hold the thermoelectric device (Fig. 3b). Under solar light densities of 1, 2, and 5 suns, a temperature difference of approximately 3.8 °C, 7.1 °C, and 14.9 °C was generated on both sides of the TE module (Fig. 3c). Correspondingly, the maximum open circuit voltages generated by the thermoelectric device are approximately 38.7 mV, 45.4 mV, and 97.4 mV, respectively (Fig. 3d). Compared with the blank hydrogel thermoelectric module exposed to one sunlight density (temperature difference = 1.7 °C, voltage = 22.6 mV), the LTL/H performance was much better than that of the uncoated thermoelectric device, with the temperature difference increased by about 2.2 times and the maximum open circuit voltage increased by about 1.7 times, confirming the feasibility of the LTL/H to improve thermoelectric power generation. It was found that under continuous solar irradiation, the voltage produced by the water-electricity cogeneration device increased rapidly within two minutes and reached a stable state at three minutes. The temperature difference curves during the thermoelectric power generation under different solar radiation densities are demonstrated as shown in Fig. 3e, which clearly compares the temperatures between the hot and cold ends of the thermoelectric sheet. Simultaneously, under 1.0 kW m<sup>-2</sup> simulated solar irradiation, the water-electricity integrated device achieved a water evaporation rate of 0.83 kg m<sup>-2</sup> h<sup>-1</sup> and a vapour conversion efficiency of 57.9% (Fig. 3f). More interestingly, these experimental results show that the photothermal conversion of the LTL/H and the water cooling coupled with the TE module can be effectively used for collaborative



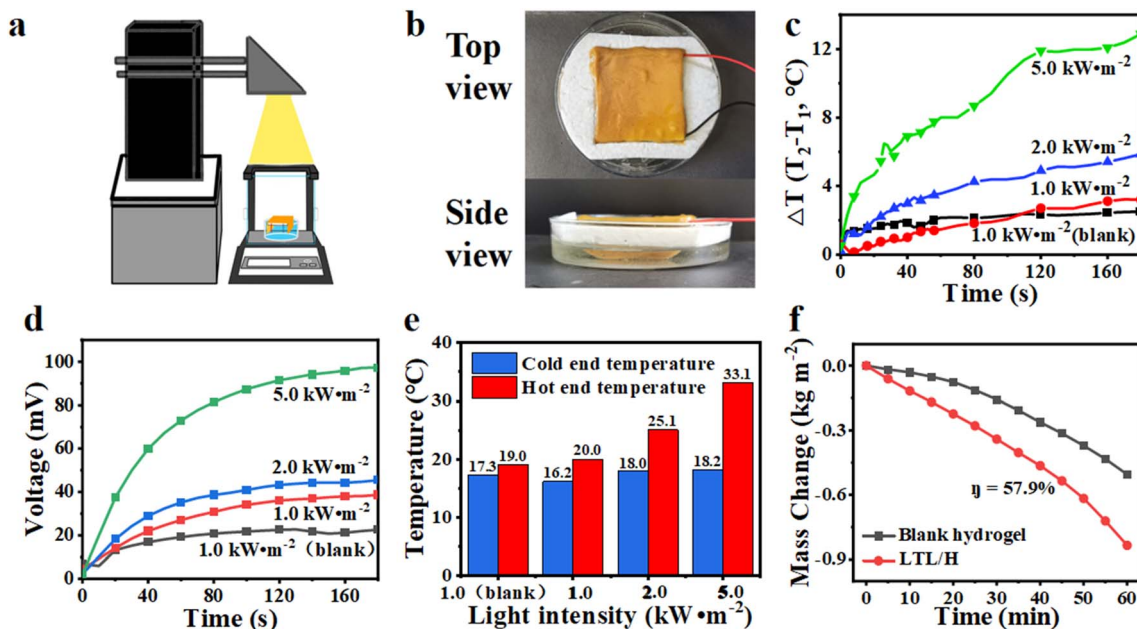


Fig. 3 (a) Schematic illustration of water evaporation and cogeneration integrated device diagram. (b) Water-electricity cogeneration device. Top and side views of the actual device can be seen in the image. PS foam was utilized as the floating carrier. (c) Temperature difference between the two sides of the LTL/H device under different solar light densities. (d) Open circuit voltage under different solar densities. (e) Temperature difference histogram of LTL/H device under different sunlight densities. (f) Weight change curves of blank hydrogel and the LTL/H over 1 h under simulated solar irradiation of  $1.0 \text{ kW m}^{-2}$ .

thermoelectric power generation, providing potential opportunities for freshwater resources and power supply in remote areas. According to the comprehensive experimental investigation results, combined water and electricity cogeneration can fully use the waste heat in solar thermal evaporation water to achieve energy diversification and reduce dependence on a certain energy source. The use of LTL/H to build solar evaporators has achieved the transportation of water and simulated its future practical application in the water environment,<sup>43</sup> and its thermal energy generation can be effectively applied to water and electricity cogeneration, achieving sustainable development in resource and energy environmental utilization research, and has broad application prospects in the field of solar photothermal conversion.

### 3 Conclusion

In summary, low-grade tobacco leaves (LTL) and polyvinyl alcohol (PVA) hydrogel were used to construct a solar steam power generation device, with good photothermal conversion performance and water evaporation ability. LTL powder has a wide absorption spectrum in the range of 300–1000 nm with a photothermal conversion efficiency of 14.33%. An eco-friendly solar-driven interfacial evaporation device was built using LTL powder as the photothermal layer and PVA hydrogel as the support carrier for water. The evaporation rate of low-grade tobacco leaves hydrogel (LTL/H) under 1 sunlight is  $1.07 \text{ kg m}^{-2} \text{ h}^{-1}$ , and the water evaporation efficiency is 74.3%. To maximize the utilization of the waste heat energy produced during evaporation, a water-electricity cogeneration device was

constructed using LTL/H and a thermoelectric module. The device aims to generate electricity based on temperature differences. The evaporation rate of the water-electric cogeneration device is measured at  $0.83 \text{ kg m}^{-2} \text{ h}^{-1}$ , with a stable output voltage of 38.7 mV under  $1.0 \text{ kW m}^{-2}$  simulated solar irradiation. The device exhibits good water evaporation and power generation performance. The results indicate that LTL is a promising solar steam power generation photothermal conversion material that can provide basic guidance for the sustainable utilization of low-grade tobacco resources and the application of seawater desalination. This newly discovered LTL/H can be used for solar-driven water and electricity cogeneration devices. This simple, efficient, and affordable way of utilizing solar energy will also provide effective solutions to the energy crisis.

### Conflicts of interest

There are no conflicts to declare.

### Acknowledgements

This work was financially supported by the Innovation Project of University Students (S202210225123), National Natural Science Foundation of China (52203212), Key Research and Development Plan Project of Heilongjiang Province (2022ZX02C13), and Special Support for Postdocs in Heilongjiang Province (LBH-TZ2215).



## References

- 1 P. Cheng, D. Wang and P. Schaaf, *Adv. Sustain. Syst.*, 2022, **6**, 2200115.
- 2 J. Eke, A. Yusuf, A. Giwa and A. Sodiq, *Desalination*, 2020, **495**, 114633.
- 3 F. E. Ahmed, R. Hashaikh and N. Hilal, *Desalination*, 2020, **495**, 114659.
- 4 J. D. Kocher and A. K. Menon, *Environ. Sci. Technol.*, 2023, **16**, 4983–4993.
- 5 D. U. Lawal, M. A. Antar, K. G. Ismaila, A. Khalifa and S. M. Alawad, *Desalination*, 2023, **548**, 116231.
- 6 S. Aly, H. Manzoor, S. Simson, M. Musnain, A. Abotaleb, J. Lawler and A. N. Mabrouk, *Desalination*, 2021, **519**, 115221.
- 7 E. J. Okampo and N. Nwulu, *Renew. Sustain. Energy Rev.*, 2021, **140**, 110712.
- 8 Z. Wang, Z. Wang, S. Lin, H. Jin, S. Gao, Y. Z. Zhu and J. Jin, *Nat. Commun.*, 2018, **9**, 2004.
- 9 D. F. Wang, S. Qi, J. W. Dong, X. Wang, Y. Zhang, S. Y. Zhou, P. Y. Gu, T. Jia and Q. C. Zhang, *Org. Lett.*, 2023, **25**, 5730–5734.
- 10 Y. Wang, W. Xu, X. Zou, L. F. Wang, Y. M. Xiang, Y. J. Jing, Q. Z. Yi, S. Ramakrishna, Y. Sun and Y. Q. Dai, *J. Mater. Chem. A*, 2023, **11**, 7422–7431.
- 11 P. Sun, W. Wang, W. Zhang, S. Zhang, J. Gu, L. Yang, D. Pantelic, B. Jelenkovic and D. Zhang, *ACS Appl. Mater. Inter.*, 2020, **12**, 34837–34847.
- 12 X. M. Cui, Q. F. Ruan, X. L. Zhuo, X. Y. Xia, J. T. Hu, R. F. Fu, Y. Li, J. F. Wang and H. X. Xu, *Chem. Rev.*, 2023, **123**, 6891–6952.
- 13 B. Shao, Y. Wang, X. Wu, Y. Lu, X. F. Yang, G. Y. Chen, G. Owens and H. L. Xu, *J. Mater. Chem. A*, 2020, **8**, 11665–11673.
- 14 X. Huang, Y. H. Yu, O. L. de Llergo, Z. D. Cheng and S. M. Marquez, *RSC Adv.*, 2017, **7**, 9495–9499.
- 15 W. Li, Z. Li, K. Bertelsmann and E. D. Fan, *Adv. Mater.*, 2019, **31**, 1900720.
- 16 G. Chen, J. Sun, Q. Peng, Q. Sun, G. Wang, Y. J. Cai, X. G. Gu, Z. G. Shuai and B. Z. Tang, *Adv. Mater.*, 2020, **32**, 1908537.
- 17 N. S. Fuzil, N. H. Othman, N. H. Alias, F. Marpani, M. H. D. Othman, A. F. Ismail, W. J. Lau, K. Li, T. D. Kusworo, I. Ichinose and M. M. A. Shirazi, *Desalination*, 2021, **517**, 115259.
- 18 E. J. Tervo, W. A. Callahan, E. S. Toberer, M. A. Steiner and A. J. Ferguson, *Cell. Rep. Phys. Sci.*, 2020, **1**, 100258.
- 19 X. Liu, Y. Tian, A. Caratenuto, F. Chen and Y. Zheng, *Adv. Eng. Mater.*, 2023, **25**, 2300778.
- 20 I. Ibrahim, V. Bhoopal, D. H. Seo, M. Afsari, H. K. Shon and L. D. Tijing, *Mater. Today Energy*, 2021, **21**, 100716.
- 21 A. Ghasemi, P. Heidarnajad and A. Noorpoor, *J. Clean. Prod.*, 2018, **196**, 424–437.
- 22 Y. Liu, J. X. Dong, G. J. Liu, H. N. Yang, W. Liu, L. Wang, C. X. Kong, D. Zheng, J. G. Yang, L. W. Deng and S. S. Wang, *Bioresour. Technol.*, 2015, **189**, 210–216.
- 23 L. A. Wallbank, R. MacKenzie and P. J. Beggs, *Ambio*, 2017, **46**, 361–370.
- 24 M. Banožić, J. Babić and S. Jokić, *Ind. Crop. Prod.*, 2020, **144**, 112009.
- 25 E. L. Terpugov, O. V. Degtyareva and V. V. Savransky, *Phys. Wave Phenom.*, 2019, **27**, 13–19.
- 26 Z. Liu, B. Wu, B. Zhu, Z. Chen, M. Zhu and X. Liu, *Adv. Funct. Mater.*, 2019, **29**, 1905485.
- 27 A. V. Ruban, R. Berera, C. Illoia, I. H. M. van Stokkum, J. T. M. Kennis, A. A. Pascal, H. van Amerongen, B. Robert, P. Horton and R. van Grondelle, *Nature*, 2007, **450**, 575–578.
- 28 C. S. Foote, Y. C. Chang and R. W. Denny, *J. Am. Chem. Soc.*, 1970, **92**, 5216–5218.
- 29 H. A. Frank, V. Chynwat, R. Z. B. Desamero, R. Farhoosh, J. Erickson and J. Bautista, *Pure Appl. Chem.*, 1997, **69**, 2117–2124.
- 30 S. Nandy, T. Hisatomi, T. Takata, T. Setoyama and K. Domen, *J. Mater. Chem. A*, 2023, **11**, 20470–20479.
- 31 T. Liu and M. S. Mauter, *Joule*, 2022, **6**, 1199–1229.
- 32 J. Gui, C. Li, Y. Cao, Z. X. Liu, J. S. Yin, H. Wei and X. L. Tian, *Nano Energy*, 2022, **107**, 108155.
- 33 S. Mao, A. Feng, X. S. Zhang, C. Onggowarsito, Q. Chen, D. Su and Q. Fu, *J. Mater. Chem. A*, 2023, **11**, 23062–23070.
- 34 L. Li, P. Wu, F. Yu and J. Ma, *J. Mater. Chem. A*, 2022, **10**, 9215–9247.
- 35 L. Bonetti, L. D. Nardo and S. Farè, *Soft Matter*, 2023, **19**, 7869–7884.
- 36 P. J. Moncure, Z. C. Simon, J. E. Millstone and J. E. Laaser, *J. Phys. Chem. B*, 2022, **126**, 4132–4142.
- 37 K. T. Campbell, K. Wysoczynski, D. J. Hadley and E. A. Silva, *ACS Biomater. Sci. Eng.*, 2019, **6**, 308–319.
- 38 X. Han, G. Xiao, Y. Wang, X. Chen, G. Duan, Y. Wu, X. Gong and H. Wang, *J. Mater. Chem. A*, 2020, **8**, 23059–23095.
- 39 M. Chazaux, C. Schiphorst, G. Lazzari and S. Caffarri, *Plant J.*, 2022, **109**, 1630–1648.
- 40 X. P. Zhao, C. X. Huang, D. Xiao, P. Wang, X. F. Luo, S. X. Liu, S. J. Li and Z. X. Chen, *ACS Appl. Mater. Interfaces*, 2021, **13**, 7600–7607.
- 41 Q. Zhang, C. L. Yang, M. S. Wang and X. G. Ma, *Mater. Today Commun.*, 2021, **26**, 101971.
- 42 Y. Zhang, Y. J. Heo, M. Park and S. J. Park, *Polymers*, 2019, **11**, 167.
- 43 M. H. Shen, X. P. Zhao, L. Han, N. X. Jin, Z. Y. Wang, S. Liu, T. Jia, Z. J. Chen and X. H. Zhao, *Chem.–Eur. J.*, 2022, **28**, e202104137.

